Scientia Iranica, Vol. 4, Nos. 1&2, pp 71–76

SCIENTIA
IRANICA

Research Note

Modification of Plasma Confinement Using Resonant Helical Fields(RHFs) on the IR-T1 (Iran-Tokamak 1)

M. Ghoranneviss*, A. Abbaspour[1], A. Anvari[2] and M. Masnavi[1]

In this article, the results of an experimental study on sawtooth instability occurring in the IR-T1 machine during an ohmic heating discharge have been presented. Different diagnostic methods, including an array of soft x-ray detectors, visible spectrometer and the electromagnetic measurement systems have been used and the intensity of visible line emissions from oxygen(OII), carbon (CIII)-impurities and Hα have been measured with and without use of resonant helical fields. The results show that the presence of some resonant helical fields, $\ell = 2$ and $\ell = 3$, could substantially modify the sawtooth oscillations and thus improve the confinement properties.

INTRODUCTION

Experiments have been performed on the IR-T1 to investigate the influence of magnetic perturbations on confinement. The perturbations are imposed via some external helical windings. A number of tokamaks have utilized a variety of helical perturbations to influence the magnetohydrodynamic activities [1]. In particular, the $m/n = 2/1$ and $m/n = 1/1$ (where m and n are poloidal and toroidal mode numbers, respectively) oscillations may be stopped, even with a very simple coil system [2-9]. On the Pulsator [10] and Tosca tokamaks [11], which have a complete set of $\ell = 2$ helical windings, a sufficiently high helical field can substantially suppress the magnetic perturbations. Also, on ATC [12] and To-1 [13], mode suppression and mode locking experiments have been performed with the help of saddle-shaped or local helical winding sets.

It has been known for a long time that the MHD equilibrium of a tokamak is subject to various forms of instability whose growth rates depend on the local values of the plasma pressure gradient, magnetic shear, current density etc. These give rise to perturbations which have the general form of:

$$\xi = \xi_0 \exp[i(m\theta - n\phi + \omega t)], \qquad (1)$$

where θ and ϕ are poloidal and toroidal angles, respectively. If m and n are small integers, satisfying the relation $q(r) = m/n$, then the surfaces are known as 'rational surfaces'. The value of q at plasma boundary, $r = a$, is often called the 'safety factor'.

The precise nature of the instabilities and the resultant perturbations depends strongly on the actual radial profiles of the various plasma parameters. For instance, if the current density near the hot center of the plasma is sufficiently high so that $q(0) < 1$, that region can support kink modes (e.g., $m/n = 1/1$) which cause the plasma to transport rapidly away from the center. This leads to a characteristic relaxation process, known as 'sawtooth' which can be seen from the shape of the oscillogram of soft x-ray emission [14,15].

In the theoretical model of the sawtooth proposed by Kadomtsev, the temperature at the plasma center increases slowly during the ramp phase because of ohmic heating. As resistive heating continues, the increase in electron temperature produces a decrease in resistivity; this leads to an increase in the current and a corresponding reduction in the safety factor q ($q = rB_t/RB_P$, where R, r, B_t and B_P are major and minor radii, toroidal and poloidal fields, respectively) to a value less than unity at the center of the plasma. This leads to an $m = 1$ instability which is observed as

*. *Corresponding author, Plasma Physics Research Center of Islamic Azad University, Tehran, I.R. Iran.*
1. *Plasma Physics Research Center of Islamic Azad University, Tehran, I.R. Iran.*
2. *Department of Physics, Sharif University of Technology, Tehran, I.R. Iran.*

a precursor to the rapid sawtooth collapse phase [2,16-18].

DESCRIPTION OF INSTRUMENTS

The IR-T1 is a small air-core transformer tokamak with circular cross section and no conducting shell and divertor. Its aspect ratio R/a is 45 cm/12.5 cm. The $q(a)$ in the machine is 3 to 7 ($q(a)$ is the safety factor in the plasma edge).

Two helical windings with optimized geometry are wound around the vacuum chamber. The minor radus of these two windings is 22 and 23 cm, respectively. Figure 1 shows the schematic structure of RHFs ($\ell = 2$, $\ell = 3$) on IR-T1. In the experiments conducted here the current through the $\ell = 2$ and $\ell = 3$ helical windings was between 100-400 A, which is very low compared with the plasma current itself (10-40 kA). The magnitudes of the RHFs were normally about 0.5-0.01% of that of the poloidal field (B_P) around the resonant surface. The length and the magnitude of the pulse feeding the helical windings could be programmed.

The main diagnostics used were: an array of Au-Si soft x-ray detectors, a visible spectrometer and electromagnetic measurement systems. The raw data were sent to a data acquisition computer through a common A/D CAMAC system and then were analyzed by a central computer.

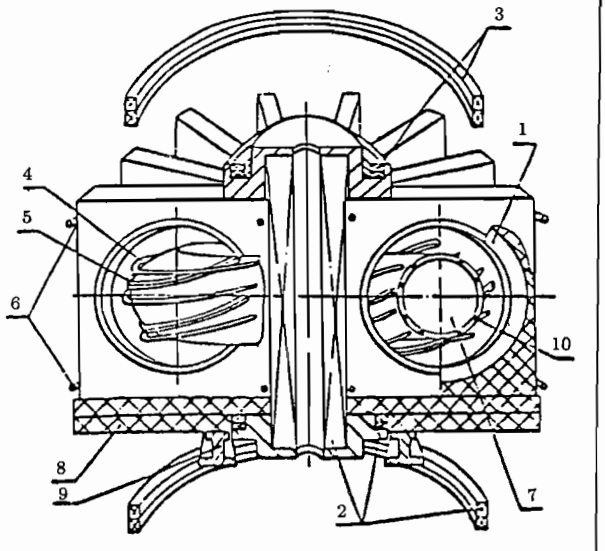

1) Toroidal field coil; 2) OH transformer coils; 3) Programable vertical field coils; 4) Helical wires $\ell = 3/n = 1$; 5) Helical wires $\ell = 2/n = 1$; 6) Horizontal field wires; 7) Vacuum vessel; 8) Bottom supporting plate; 9) Guides; 10) Feed back vertical field coils.

Figure 1. Schematic view of RHF of IR-T1.

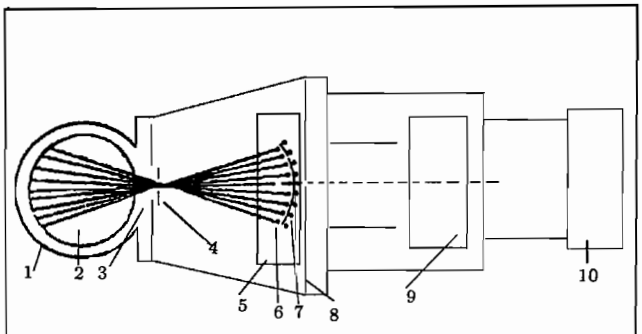

1) Vacuum chamber; 2) Plasma; 3) Window; 4) Absorption film; 5) Collimating shield cover; 6) Detector array; 7) Preamplifier; 8) Detector chamber; 9) Amplifier filter; 10) Data collector and processor.

Figure 2. Soft x-ray emission-measurement system of IR-T1.

Soft X-Ray Emission-Measurement System of IR-T1.

The soft x-ray measurement system includes four subsystems, namely: detection chamber, silicon detector array, filter circuit and data collection system.

Figure 2 shows the construction of the system. An array surface barrier detector (Ortec TB-18-25-300) is located at a place facing the center of the vacuum chamber; the detectors are able to detect soft x-ray signals from different parts of the chamber.

The detector array, which is installed in a horizontal location, consists of 23 silicon barrier diodes. It also consists of 13 similar diodes which were installed in a vertical position. The sensitive area of each detector element is about 50 mm^2. The energy range of the detected soft x-ray is about 600 ev to 20 kev. The detector chamber is insulated from the vacuum chamber and the collimating shield cover is also insulated from the detector chamber. An absorption film, 3μm thick made of formver with aluminum coating (4000 $\AA$ thick), is used to block the visible and vuv radiations.

The signals from the detector are digitized with 12 bit accuracy by means of a data acquisition system. The memory allocation for this unit (256 kilo-words) is large enough such that 25 ms of the pulse (which in general includes all interesting features) can be properly acquired even at a 200 kHz sampling rate.

Visible Spectrometer System

The profiles of visible line emissions from OII (λ = 4416 $\AA$, $2p^2 3s$-$2p^2 3p$), CIII (λ = 4644 $\AA$, 2s3s-2s3p)-impurities and Hα (λ = 6563 $\AA$, 3-2) line have been determined using a visible spectrometer, in which there is a two-lens image system in front of its entrance slit and a multichannel optical fiber attached to its exit slit. The detectors in this system are photomultipliers.

EXPERIMENTAL OBSERVATIONS

The typical time evolutions of plasma parameters under the following conditions are shown in Figure 3a-d. These parameters are the plasma current, loop voltage, soft x-ray signal and the safety factor of the plasma edge, respectively. In this paper, convention has been followed by defining q(a) in its cylindrical approximation [15,19]:

$$q(a) = 2\pi B_t a^2/\mu_0 I_p R \ . \qquad (2)$$

Here, R, a, B_t and I_p are the major and minor radii in meters, the toroidal field in Tesla and the plasma current in Ampers, respectively. The following is a list of parameters:

Plasma current

$$28 \leq I_p \leq 45 \text{ kA}$$

Toroidal field

$$0.57 \leq B_t \leq 0.75 \text{ T}$$

Pulse duration

$$18 \leq T \leq 22 \text{ ms}$$

Central electron temperature

$$100 \leq T_e(0) \leq 185 \text{ ev}$$

Line average central electron density

$$1 \leq n_e \leq 2.3 \times 10^{13} \text{ cm}^3$$

Effective ion charge

$$1 \leq \text{Zeff} \leq 2.2$$

Confinement time (Goldston scaling)

$$0.5 \leq \tau e \leq 2.5 \text{ ms}$$

The sawtooth inverse phase radius (r_0)

$$2.2 \leq r_0 \leq 3.5 \text{ cm}$$

The sawtooth period (τs)

$$250 \leq \tau s \leq 430 \ \mu\text{s}$$

In the above list, the effective ion charge (Zeff) has been calculated using the classical Spitzer parallel resistivity defined as [15]:

$$\eta s = 36.04 \times 10^{-5} \text{ Zeff}[1 + 1.56/(1.08 + \text{Zeff})] \times Te^{-3/2} \text{ (ev)} \ . \qquad (3)$$

Furthermore, the global energy confinement time (τ_e) is obtained according to the definition of the empirical Goldston scaling law [15]:

$$\tau_e(\text{second}) = 1.0 \times 10^{-21} n_e a R^2 q(a)^{0.5}. \qquad (4)$$

The radius of the $q = 1$ surface has been derived from the resulting data and also from calculating the sawtooth inverse phase radius r_0, using the following empirical relation:

$$r_0 = 0.5 \times a/\sqrt{q(a)} \ , \qquad (5)$$

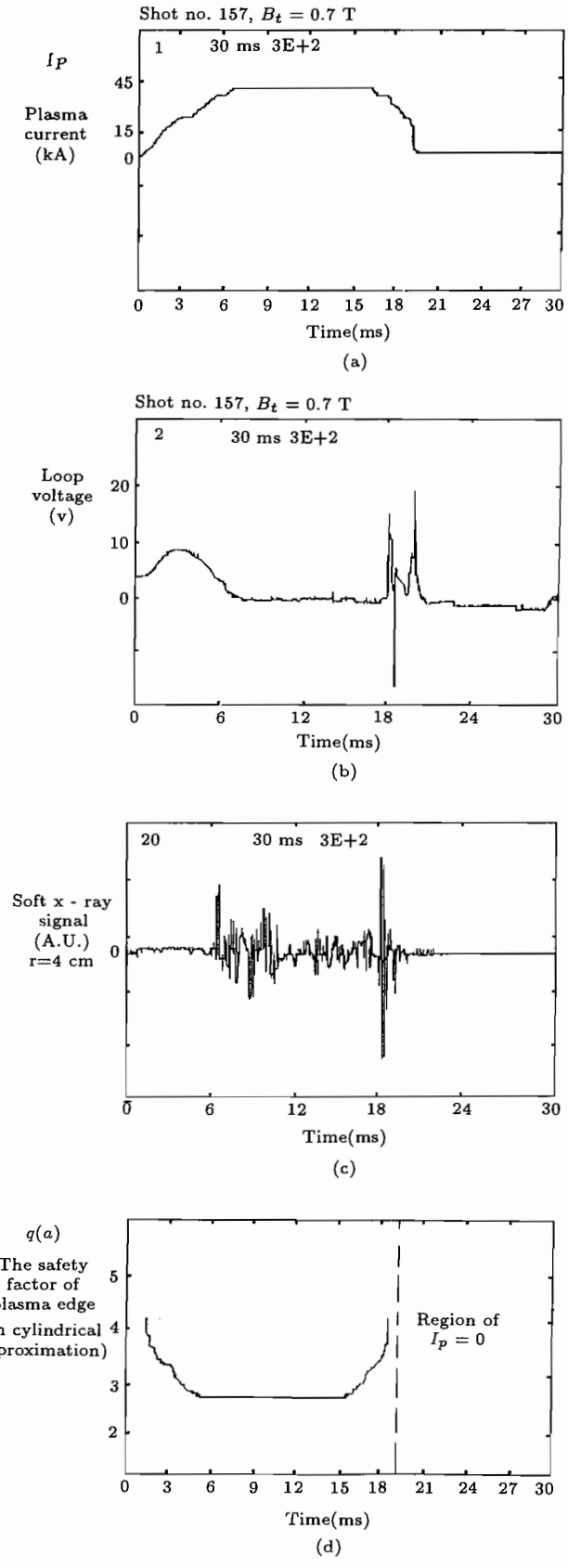

Figure 3. (a) Plasma current (b) Loop voltage (c) The soft x-ray emission signal and (d) Safety factor of plasma edge.

which were quite in agreement . The sawtooth period (τs) has been derived from the soft x-ray signals using the empirical relation given below [18,19]:

$$\tau_{\text{sawtooth}}(\text{sec.}) = 10^{-2} R^2(\text{m}) T_e^{3/2}(\text{kev})/\,\text{Zeff}. \qquad (6)$$

As can be seen in Figure 3, in the first 5 ms of the plasma current, no remarkable soft x-ray signals exist. This is because plasma current, as seen in Figure 3a is about 23 kA and the loop voltage is around 4-8 v. This leads to a central electron temperature of about $T_e(0) < 100$ ev. According to Figure 3c, the fluctuation of soft x-ray signals has started after 5 ms in which the loop voltage has decreased to its flat situation. Figure 3d shows the safety factor profile as calculated by means of Figure 3a.

The effects of $\ell = 2$ and $\ell = 3$ RHFs on sawtooth oscillations have been studied only in the plateau phase (6 to 17 ms) of the plasma current. Figure 4a shows the effect of $\ell = 2$ RHF ($I_\ell \approx 400$ A) on soft x-ray emission, between 10 to 15 ms, corresponding to the first flat part of plasma current (Figure 4b). This shows an increase in period of sawtooth oscillations which in turn indicates more stable conditions.

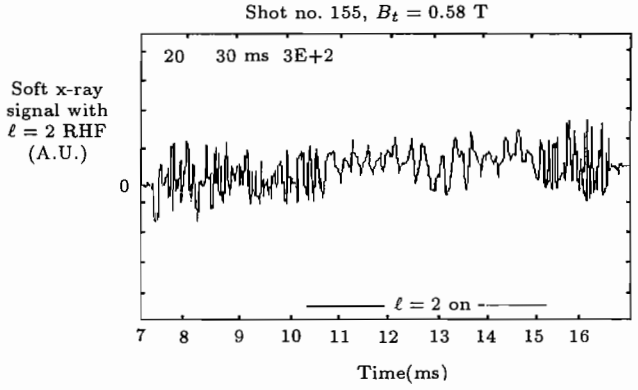

Figure 4a. The SXR emission measured along the chord ($r = +1$ cm, where r is distance from the torus center), $m = 1$ fluctuation is suppressed by $\ell = 2$ RHF.

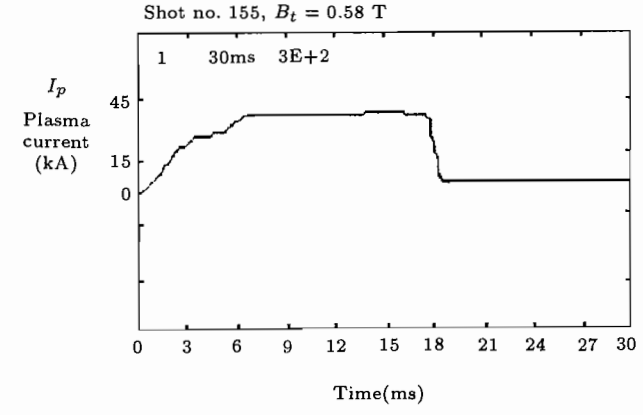

Figure 4b. Plasma current with RHF.

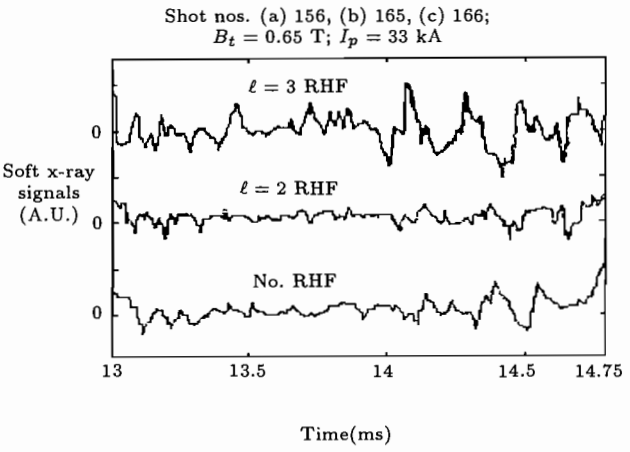

Figure 5. Sawtooth behavior with RHFs, curves from the top are SXR at +3 cm, (a) with $\ell = 3$, (b) $\ell = 2$ and (c) without RHFs .

Figure 5 compares three soft x-ray signals, obtained with RHFs under the condition of $I_\ell \approx 140$ A, showing the effect of using (a): $\ell = 3$ RHF, (b) $\ell = 2$ RHF and (c): without RHF. In this case, the sawtooth instability for $\ell = 2$ is lower in comparison with that of the two others because the plasma current is lower than that of Figure 4.

As can be seen from the above results, it is found that the $\ell = 3$ RHF has very effectively modified sawtooth oscillations when q(a) is close to 4. On the other hand, the $\ell = 2$ is more effective in range of q(a) ≤ 3.5.

The spectral visible line emissions of the light impurity ions were also investigated. Figures 6–8 show the measurement results of visible line emissions of OII, CIII-impurities and Hα with and without RHF ($\ell = 2$). The amplitude of visible line emissions of light impurities (OII and CIII) and Hα held a plateau while RHF was on . The visible line emissions from both oxygen and carbon impurities is much lower

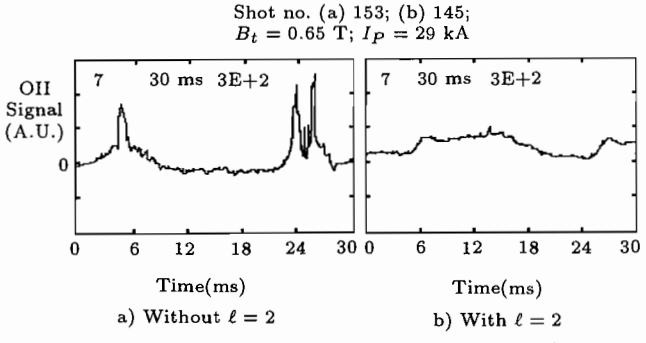

Figure 6. Line emission signals of OII (+3.56 cm).

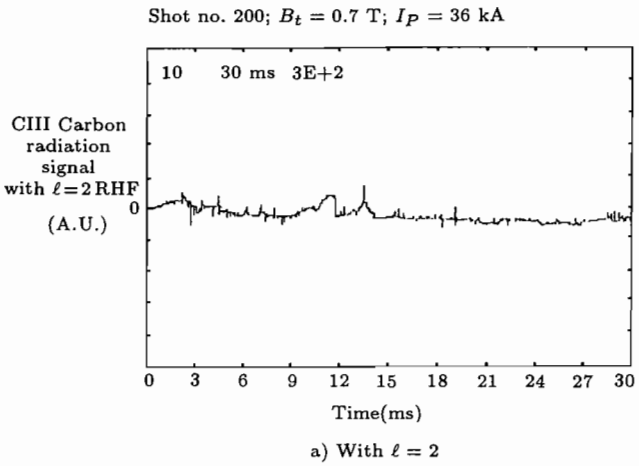

a) With $\ell = 2$

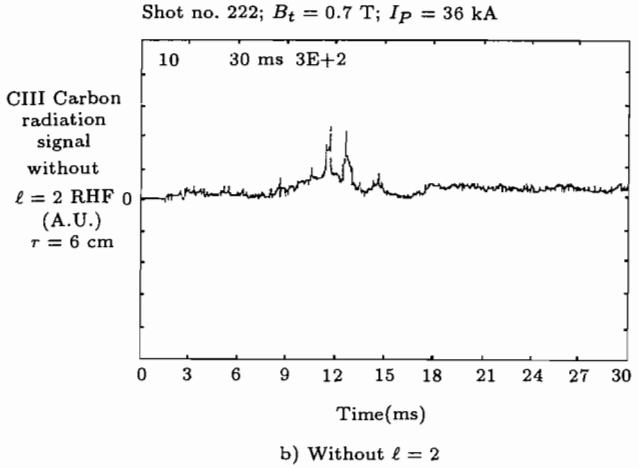

b) Without $\ell = 2$

Figure 7. Visible line emissions of CIII (+6 cm).

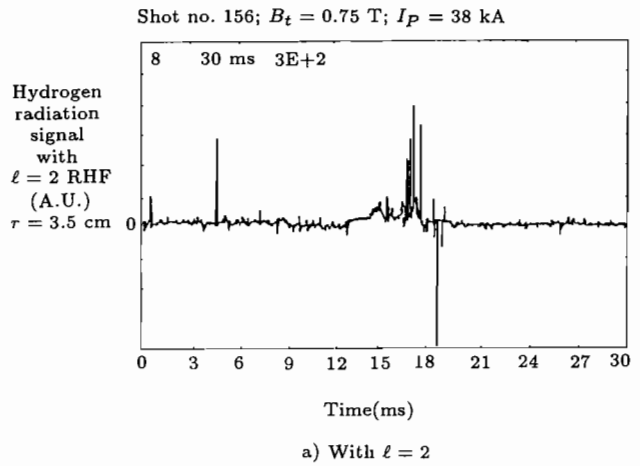

a) With $\ell = 2$

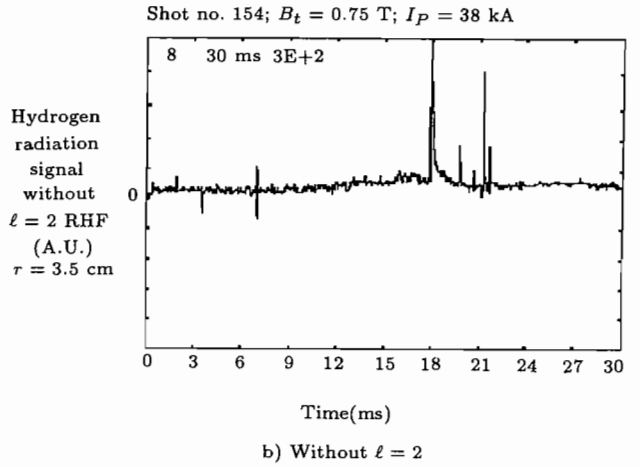

b) Without $\ell = 2$

Figure 8. Visible line emissions Hα (+3.56 cm).

than its value obtained without RHF. On the other hand, the emissions of OII and CIII-impurities are completely distributed over the whole range of the plasma duration.

As shown, the Hα radiation does not behave as OII and CIII-impurities during the RHF period and is not enhanced over the whole range of plasma duration by RHFs (hydrogen influx was unchanged). This shows that the RHFs have no influence on the main particles of the plasma [20].

CONCLUSION

The stability properties of the discharges are improved using resonant helical fields as indicated by an increase in the period of sawtooth oscillation and, also, by a better distribution of emissions of OII and CIII impurities radiations over the whole range of the discharge duration. However there is no remarkable influence on the Hα radiations. These results show that the $\ell = 3$ RHF is very effective on sawtooth oscillations when the safety factor in plasma edge q(a) is close to 4, while the $\ell = 2$ is more effective in range of $q(a) \leq 3.5$.

ACKNOWLEDGMENTS

The authors would like to thank the technical staff of the laboratory for their kind collaboration and, in particular, M.Z. Mehr for his efforts in handling the data acquisition system.

REFERENCES

1. Ellis, J.J. and Morris, A.W., "Resonant helical fields on tokamaks", *Controlled Fusion and Plasma Physics, Proc. of 11th Europ. Conf.*, Aachen, Germany, **15**(1), paper O4 (1983).
2. Huo, Y.P. "Tearing modes in tokamak plasmas", *Small Plasma Physics Experiments II Conference*, ICTP Trieste, IAEA, Italy, pp 52–89 (1989).
3. Linzhong, Li. "Tearing modes on tokamaks", Chinese Science, **3**, pp 284–290 (1990).

4. HT-6B Group, "MHD behaviour of the HT-6B tokamak with a weak helical current perturbation", Report ASIPP/11, Institute of Plasma Physics, Academia Sinica, Hefei (1985).

5. Chen, Jiayu, "Global structure of MHD modes in tokamaks", *Nuclear Fusion*, **30**(11), pp 298-337 (1990).

6. Rong, Huang and Xie Jikang, "Spectroscopic diagnostics in the HT-6B Tokamak", Academia Sinica, ASIPP/126, pp 1-10 (1991).

7. Xie Jikang, "Modification of sawtooth behavior using RHF on HT-6B tokamak", *Proc. 14th Euro. conf.*, Madrid, Spain, **1**, pp 221-227 (1987).

8. Xie Jikang, "Studies of MHD modes and high frequency fluctuations on the HT-6B and HT-6M tokamaks", *Plasma Physics and Controlled Nuclear Fusion Research IAEA-CN-47/A-V-6h*, **1** (1986).

9. Zhaoa, Q. "Suppression of tearing modes in tokamaks by a helical magnetic field", *Plasma Physics and Controlled Nuclear Fusion Research IAEA- CN-44/A-V-5-3*, **1**, pp 345-353 (1985).

10. Karger, F. and Wobig, H. "The origin of the disruptive instability in the pulsator tokamak", *Plasma Physics and Controlled Nuclear Fusion Research IAEA*, Tokyo, Japan, **1**, pp 207-215 (1975).

11. Ellis, J. and Howling, A. "The influence of resonant helical fields on tokamak confinement", *Plasma Physics and Controlled Nuclear Fusion Research IAEA*, **1**, London, UK, pp 363-370 (1985).

12. Bol, K. "Resonant helical fields", *Plasma Physics and Controlled Nuclear Fusion Research IAEA*, Tokyo, Japan, **1**, pp 83-90 (1975).

13. Arsenin, V. and Artemenkov, L., "Mode suppression by RHF in To-1 tokamak", *Plasma Physics and Controlled Nuclear Fusion Research IAEA*, Innsbruck, **1**, pp 233-240 (1979).

14. Avinash, K. and Hastie, R.J. "Sawtooth oscillation", *Phys. Rev. Lett.*, **59**, pp 2647-2651 (1987).

15. Wesson, J. *Tokamaks*, Clarendon press, London, UK, pp 160-180 (1986).

16. Campbell, D.J. and Wesson, J.A. "Sawtooth activity in ohmically heated JET plasmas", Nuclear Fusion, **26**(8), pp 1085-1092 (1986).

17. Costley, A.E. "Diagnostic advances and their impact on our understanding of tokamak relaxation phenomena", *Plasma Physics and Controlled Fusion*, **30**(11), pp 1455-1466 (1988).

18. Monticello, D.A., Park, W. and McGuire, K. "A review of calculation of the resistive internal m=1 modes in tokamaks", *Computer Physics Communications*, **43**, pp 57-67 (1986).

19. Equipe TFR "Tokamak plasma diagnostics", *Nuclear Fusion*, **18**(5), pp 647-730 (1978).

20. Ghoranneviss, M. and Masnavi, M., "Modification of plasma confinement by using resonant helical fields in IR-T1 Tokamak", *23rd European Physical Society Conference On Controlled Fusion and Plasma Physics*, Kiev, Russia (June 24-28, 1996).